Springer

KSME

Journal of Mechanical Science and Technology 32 (7) (2018) 3419~3425
www.springerlink.com/content/1738-494x(Print)/1976-3824(Online)
DOI 10.1007/s12206-018-0645-3

Simulation of temperature rise within a rolling tire by using FE analysis †

Hyun Seok Song[1], Sung Pil Jung[2] and Tae Won Park[3,*]

[1]*Extream Technology R&D Center, Korea Automotive Technology Institute, Cheonan 31214, Korea*
[2]*Premium Car R&D Center, Korea Automotive Technology Institute, Younaam 58463, Korea*
[3]*Department of Mechanical Engineering, Ajou University, Suwon 16499, Korea*

(Manuscript Received May 25, 2017; Revised January 9, 2018; Accepted March 21, 2018)

Abstract

A simulation method is proposed to predict temperature rise within a dynamic rolling tire. The friction heat from tire-road contact and the internal heat generated by hysteresis loss caused by rubber deformation are considered in the simulation model. A systematic process was developed to calculate the heat generation rate by using dissipated energy, and it was applied to the simulation model by establishing user subroutines. An axial tensile test was conducted for the rubber specimen, and the obtained stress-strain curve was applied to the simulation model based on the first-invariant Marlow model. The reliability of the simulation method was verified by comparing the tensile simulation and test results. A simplified 3D finite element tire model was developed, and simulations were performed in dynamic rolling conditions. Heat was generated because of friction and internal deformation. The temperature distribution within the tire, which was derived using the model, indicates that the proposed simulation method is reliable.

Keywords: Friction heat; Internal heat; Temperature rise; Finite element tire model; Marlow model; Dynamic rolling condition

1. Introduction

Tire temperature is one of the primary parameters that affect tire durability and performance. The rubber failure properties of a tire depend on its temperature [1]. Temperature rise within a tire occurs because of two reasons: (1) Friction between treads and roads and (2) internal heat generation due to the repeated deformation of the rubber material.

Experimental studies were performed to investigate the temperature rise within the rubber material in accordance with its composition [2, 3]. However, measuring internal temperature rise within a tire is considerably difficult because the tire and its rim are assembled by using high air pressure and they roll together. In this study, a method for numerical simulation is proposed to predict internal temperature rise within a tire.

Several studies have been conducted to predict tire temperature. Park [4] proposed a numerical method to predict the temperature distribution within a steady-state rolling tire. The stress and speed of the tire were both calculated using a mechanical solver. Then, the energy dissipation rate of the viscoelastic rubber material was calculated. Finally, the temperature distribution within the tire was derived using a thermal solver. However, this approach is limited because it can only be adopted only for steady-state analysis, such as rolling resistance simulation. Lin [5] proposed a similar method to predict the temperature in a tire by using sequential computer simulation. First, structural analysis was carried out using ANSYS/LS-DYNA, and the dissipative strain energy was calculated using strain-stress curve data. Then, steady-state thermal analysis was performed using ANSYS/mechanical programming.

In recent years, the direct co-simulation of structural and thermal solvers has been performed with Abaqus. Johnson [6] and Kan [7] simulated a thermo-mechanically coupled problem in cyclic loading using Abaqus. Luo [8] solved a coupling problem based on a staggered approach by combining the Abaqus user subroutines of UMASFL, USDFLD, HETVAL and UEXTERNALDB. Tang [9] predicted the temperature distribution of a steady-state rolling tire. However, these previous studies were conducted with steady-state transport analysis, in which tire deformation due to road contact is calculated as a stage only, whereas shape deformity is analyzed with other methods. Therefore, the actual deformation of a rolling tire influenced by road conditions cannot be considered, and it even causes error in estimating temperature rise.

This study proposes a simulation method by using Abaqus to predict the temperature distribution within an actual rolling tire (i.e., not a steady-state rolling tire). The USDFLD subroutine is developed to define how internal heat is generated within a rubber. In general, temperature-dependent material properties and changes in the contact condition between tread and

*Corresponding author. Tel.: +82 312192952, Fax.: +82 312191965
E-mail address: park@ajou.ac.kr
† Recommended by Associate Editor Youngsuk Nam

Fig. 1. UTM with thermal chamber and rubber specimen.

road cause the thermal expansion of tires. Simulation is therefore conducted automatically, not sequentially.

2. Simulation of internal heat generation in rubber

2.1 Marlow model

In this study, the first-invariant Marlow model [10] is used as the constitutive model for the rubber material. This model can be easily defined with uniaxial tensile testing, and it can reproduce exact test data [11]. The form of the Marlow strain energy potential [12] is

$$U = U_{dev}(\bar{I}_1) + U_{vol}(J_{el}), \tag{1}$$

where U is the strain energy per unit reference volume, with U_{dev} and U_{vol} as the deviatoric and volumetric components, respectively; $\bar{I}_1$ is the first deviatoric strain invariant; and J_{el} is the elastic volume ratio. $\bar{I}_1$ is defined using the principal stretches $\bar{\lambda}_i$ as

$$\bar{I}_1 = \bar{\lambda}_1^2 + \bar{\lambda}_2^2 + \bar{\lambda}_3^2, \tag{2}$$

where $\bar{\lambda}_i = J^{-\frac{1}{3}\lambda_i}$

2.2 Uniaxial tensile test

A universal testing machine (UTM) was used with the uniaxial tensile test. The rubber specimen was acquired from the sidewall of tires and its thickness is 2 mm in accordance with ASTMD-412-C. The load-displacement curve was determined and subsequently transformed into a nominal stress and strain curve. Fig. 1 shows the UTM with the thermal chamber and specimen. To determine the variations in tensile characteristics with temperature, the temperature within the chamber was changed. Table 1 shows the test conditions. The specimen was kept for five hours, cyclic loading was applied three times at each temperature point, and the averages of the stress and strain were used as representative values.

Fig. 2 shows the tensile test result. The maximum stress decreased gradually with the increase in temperature. This scenario implies that thermal deformation of the rubber specimen occurred and its strength is decreased. Stress decreased gradually when temperature changed from 25 °C to 70 °C. From 70 °C to 120 °C, the decreasing speed of the stress was reduced. Owing to hysteresis and viscoelastic characterization, the stress-strain curve differed in loading and unloading conditions. The area between the stress and strain curves corresponding to the loading and unloading conditions is referred to as energy loss or hysteresis loss. In general, energy loss causes internal heat generation, permanent deformation, and fatigue in rubber.

Table 1. Tensile test conditions.

Max. displacement	15 mm
Speed	5 mm/min
Temperature	25, 45, 70, 95, 120 °C

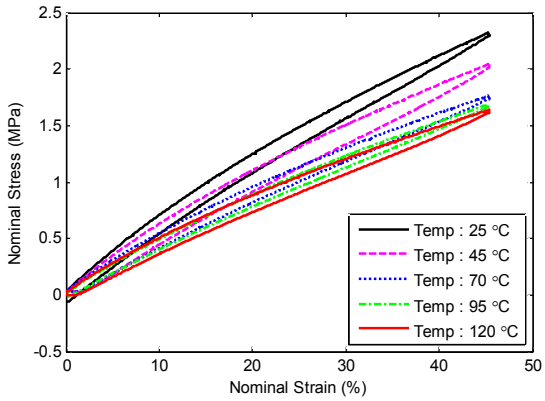

Fig. 2. Tensile test result.

2.3 Development of user subroutine

A user subroutine in Abaqus was developed to simulate internal heat generation. As shown in previous references, most studies used steady-state transport analysis method to reduce simulation time by avoiding the repetitive nonlinear contact condition. However, this approach can neither determine the actual tire deformation nor calculate the friction heat between the tire and the road. In this study, implicit dynamic analysis is conducted for tire roll on an actual road. Thus, the friction heat caused by road contact and the internal heat caused by deformation can be calculated simultaneously. Fig. 3 shows the structure of the analytical process, including the USDFLD and HETVAL user subroutines. USDFLD redefines field variables at a material point while HETVAL provides internal heat generation for heat transfer analysis [12]. The material model was defined based on the Marlow model, and its viscoelasticity was determined using the first-order Prony series based on the tensile test result shown in Fig. 2.

The material model shows how the user subroutines are initiated. USDFLD is used to calculate the total dissipated strain energy density, as expressed by

$$U_{Total} = (U_P + U_C + U_V + U_D) \times V_u, \tag{3}$$

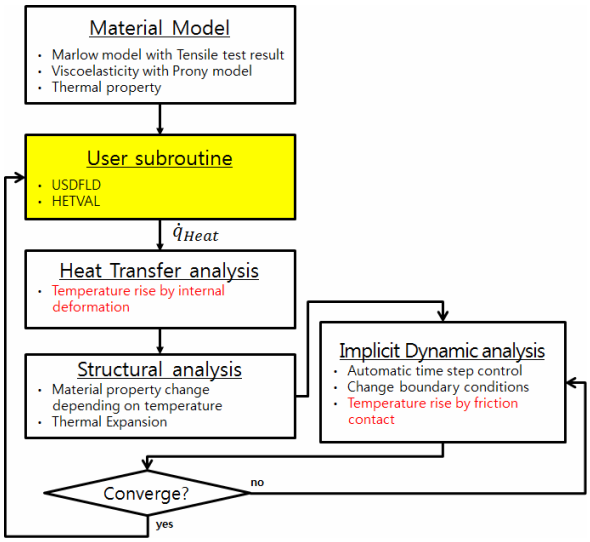

Fig. 3. Analytical process.

where U_P is the energy density dissipated by the rate-independent and rate-dependent plasticity per unit volume; U_C is the energy density dissipated by the creep, swelling, and viscoelasticity per unit volume; U_V is the energy density dissipated by the viscous effects per unit volume; U_D is the energy density dissipated by damages due to stress per unit volume; and V_u is the integration point volume. Total dissipated strain energy density is not recovered after deformation. Moreover, convection heat transfer was not considered in this study. Accordingly, total dissipated strain energy density was assumed to be fully converted into internal heat generation rate.

HETVAL is used to calculate the heat generation rate per unit volume by using total dissipated strain energy [9], such that

$$\dot{q}_{Heat} = U_{Total} \times f \ , \tag{4}$$

where f is frequency, which is defined as the longitudinal velocity (V_L) divided by the circumference of the rolling tire with radius r.

$$f = \frac{V_L}{2\pi r} \ . \tag{5}$$

The calculated heat generation rate was applied as an input condition for heat transfer analysis. The tire model was deformed due to the temperature-dependent material properties. The deformed shapes of the tire model were used as basis for structural analysis. The findings show the influence of changes in boundary conditions, including tread-road contact.

2.4 Tensile simulation

A tensile simulation model was constructed to verify the developed user subroutines. Fig. 4 shows the finite element (FE) model and its boundary conditions. The FE model was developed in accordance with ASTMD-412-C. Two reference nodes were generated and connected rigidly at each side of the model. One reference node was fully fixed, and a displacement of 15 mm with a speed of 5 mm/min was applied at the other reference node. The setup is the same as that shown in Table 1. Convection heat transfer was neglected. Table 2 shows the parameters used in the FE model and their material properties.

Table 2. FE model parameters and material properties for tensile simulation.

FE information	Number of elements	7735
	Number of nodes	5762
	Type	Hexagonal
Material properties	Density (kg/m^3)	945
	Elastic modulus (GPa)	Marlow
	Poisson's ration	
	Thermal conductivity (W/m °C)	0.14
	Specific heat (J/kg°C)	1050
	Thermal expansion coefficient (10^{-5}/°C)	1.05

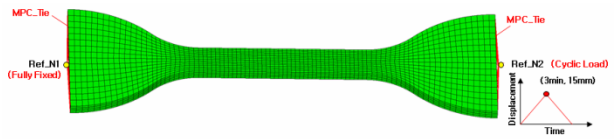

Fig. 4. Tensile simulation model.

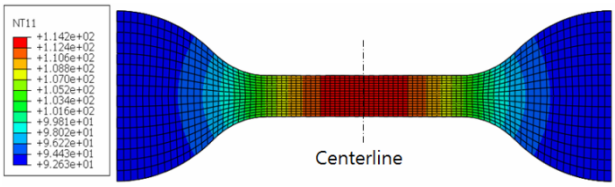

Fig. 5. Temperature distribution of the tensile simulation model after 200 loading cycles.

Fig. 5 shows the temperature distribution of the tensile simulation model after 200 loading cycles. When repetitive displacement was applied, the temperature at each node was increased. The maximum temperature reached 114.2 °C after 200 loading cycles. Fig. 6 shows the temperature rise in accordance with the longitudinal position of the specimen in which the deformation was the largest at the center. This phenomenon suggests that the temperature at the center is considerably higher than that at the end parts. The temperature deviation between the center and the end part increased when the number of loading cycles increased.

Fig. 7 shows the change in reaction force at the reference node and the maximum temperature at the centerline with the number of loading cycles. After 200 cycles, the maximum reaction force decreased by approximately 30 % from 13.9 to 9.7 N. The maximum load also decreased gradually until the temperature reached 35.1 °C after 10 loading cycles. From the

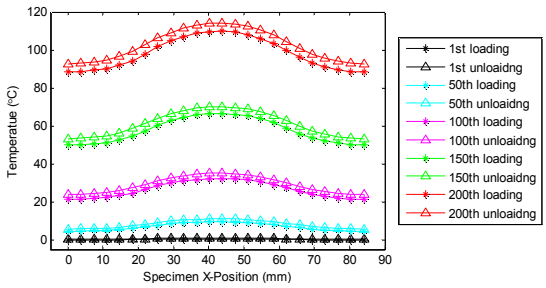

Fig. 6. Temperature deviation according to the longitudinal position of the specimen.

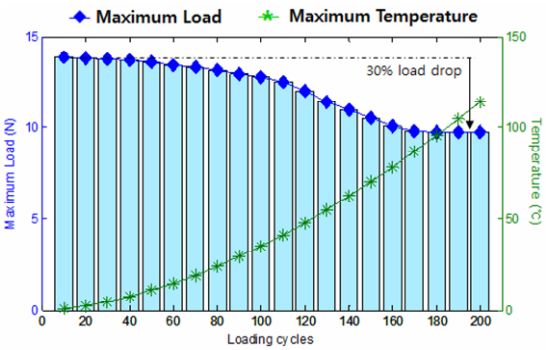

Fig. 7. Change in reaction force and maximum temperature with loading cycles.

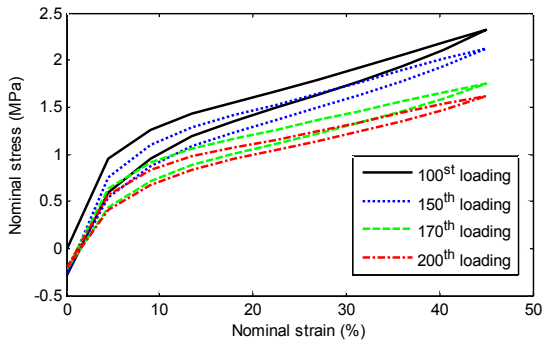

Fig. 8. Change in nominal stress of the tensile simulation model.

110th to the 160th loading cycles, the largest decrease in the maximum load was observed, and the maximum temperature is 78.2 °C. The maximum load stabilized starting the 170th loading cycle, but the maximum temperature continued to increase. This result indicates that the stiffness and durability of the rubber material are lowered by the rise in temperature.

Fig. 8 shows the hysteresis curves corresponding to the repetitively applied displacement. As the number of loading cycles increased, the nominal stress decreased. This stress scenario is similar to the trend shown in Fig. 2. For quantitative comparison, the maximum nominal stress between tensile test and simulation results were analyzed (Table 3). Only a small error of 0.02-0.07 MPa was observed, which proves that the simulation model can be used to represent the actual tensile test results.

Table 3. Comparison of maximum nominal stress between tensile test and tensile simulation based on temperature.

Temperature	Maximum nominal stress (MPa)		
	Test (A)	Simulation (B)	Error (A-B)
25 °C	2.33	2.31	+0.02
45 °C	2.05	2.12	−0.07
70 °C	1.77	1.75	0.02
120 °C	1.64	1.62	0.02

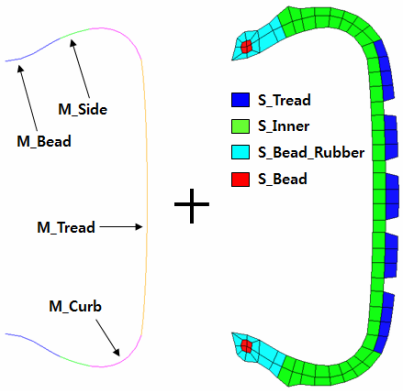

Fig. 9. Structure of the simplified tire model.

3. Heat generation in rolling tire

3.1 Tire model

In this study, a simplified tire model with 225/45R17 specifications was developed (Fig. 9). The tire model comprised 159 nodes and 148 elements, and constructed by using two types of elements, namely, solid and membrane. Four solid parts (S_tread, S_inner, S_bead and S_steel) comprise the rubber and steel material, while the four membrane parts (M_tread, M_curb, M_side and M_bead) represent the reinforcements. Table 4 shows the material properties of each part. The tread was rendered to come into contact with the road. Accordingly, isotropic material properties were used to maintain sufficient stiffness. The membrane elements have no thermal material properties.

3.2 Simulation of internal heat generation

Fig. 10 shows the boundary conditions applied to simulate internal heat generation by repetitive deformation. Four nodes on the tread that were in contact with the road were selected. The tire was attached to two rims i.e., defined as rigid surfaces, and the two reference nodes of Ref_N_Rim1 and Ref_N_Rim2 were connected rigidly to both rims. A cyclic displacement of 0-10 mm was applied to the two reference nodes. A pressure of 2.2 kgf/cm^2 was applied within the tire to generate inflation pressure. The rotational degrees of freedom of the center node of the S_bead part were fixed.

Fig. 11 shows the rise in temperature due to the internal heat generated by the repetitive deformation component of the

Table 4. Mechanical and thermal material properties of the tire model.

Mechanical material properties					
Element type	Part	Density (kg/m^3)	Elastic modulus (GPa)	Poisson's ratio	Thickness (mm)
Solid	S_tread	1000	0.007	0.48	-
	S_inner	945	Marlow model		-
	S_bead	1000	0.008	0.48	-
	S_steel	8000	800	0.3	-
Membrane	M_tread	1200	218.7	0.3	0.05
	M_curb	1200	6.78	0.3	0.01
	M_side	1200	7.83	0.3	0.01
	M_bead	1200	2.61	0.3	0.1

Thermal material properties				
Element type	Part	Thermal expansion coefficient (10^{-5}/°C)	Thermal conductivity (W/m °C)	Specific heat (J/kg °C)
Solid	S_tread	1.05	0.14	1050
	S_inner	1.05	0.14	1050
	S_bead	1.05	0.14	1050
	S_steel	1.05	53	1000

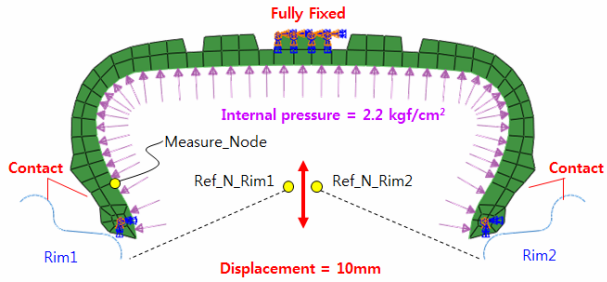

Fig. 10. Boundary conditions for repetitive compression.

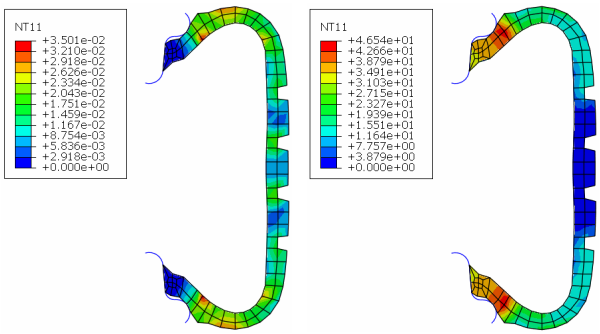

(a) 1st compression (b) 30th compression

Fig. 11. Temperature distribution by using the tire model at different loading cycles.

model. The temperature of the S_tread part was low because the nodes outside the tread were fixed and the deformation of the tread was small. The deformation of the S_inner part to which the rim was attached was the largest, and the internal

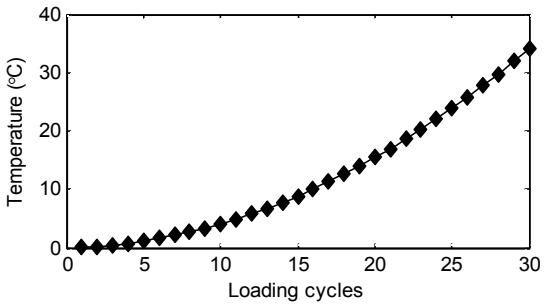

Fig. 12. Temperature rise at measure_node with number of loading cycles.

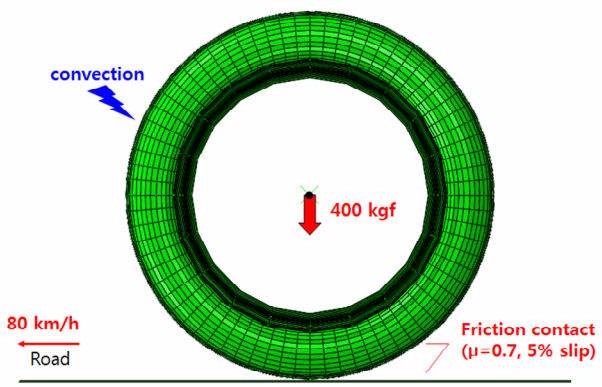

Fig. 13. 3D tire model and boundary conditions.

heat generation was concentrated in that area. After 30 cycles of compression, the maximum temperature was approximately 46.5 °C. When the rim was displaced repetitively, the temperature of measure_node (i.e., see Fig. 10) increased nonlinearly (Fig. 12). This result verified the existence of the thermal expansion corresponding to the temperature rise depicted by the Marlow model.

3.3 Simulation of temperature rise within the rolling tire

When a tire rolls on a road, two heat sources (i.e., friction heat and internal heat) can be observed. The 3D tire model in this study was developed by revolving the 2D model shown in Fig. 10. The tire model was designed to simulate the temperature rise in rolling conditions when friction heat and internal heat are applied simultaneously. Friction heat can easily be generated by using the **GAP heat generation* and **GAP conductance* protocols in Abaqus. The internal heat generation in this study was achieved using the developed user subroutine, as described in Sec. 2.3.

Fig. 13 shows the 3D tire model. A vertical load of 400 kgf was applied at the two reference nodes (Fig. 10). The road was designed to move in the longitudinal direction at the constant speed of 80 km/h. The friction coefficient and slip ratio of the tire-road contact were assumed to be 0.7 and 5 %, respectively. A convection condition was applied outside the tire.

Fig. 14 shows the temperature distribution within the rolling

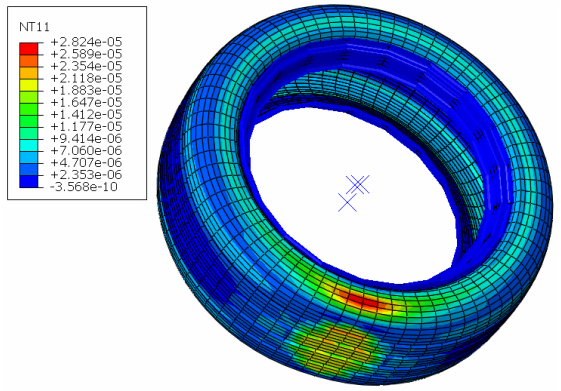

(a) First stage: Contact with the road

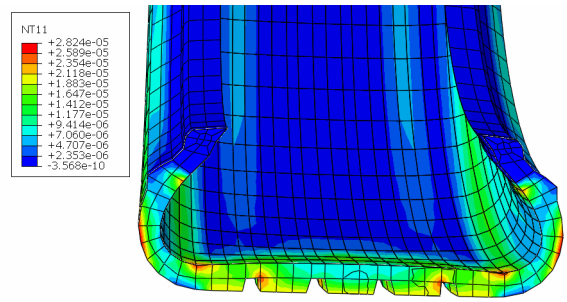

(b) First stage: Contact with the road (cut-section)

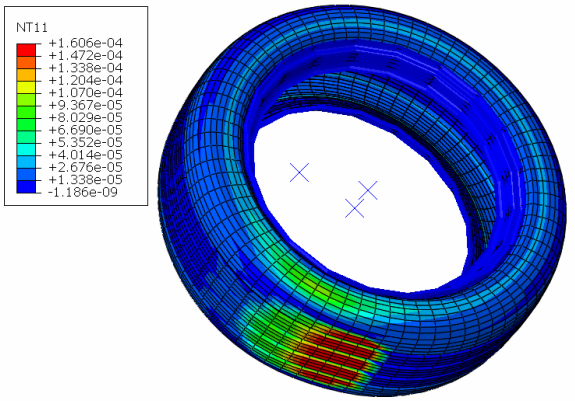

(c) Second stage: Start of rolling

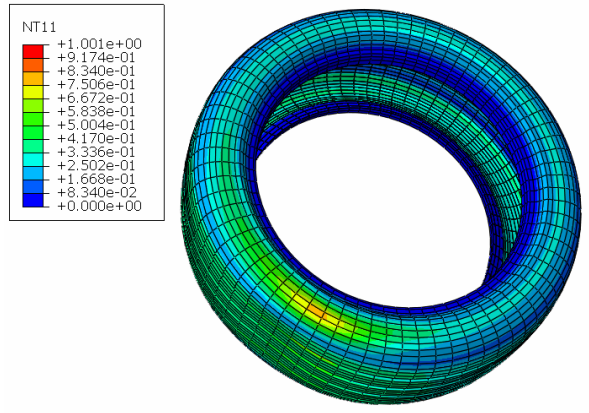

(d) Third stage: After 30 rotations at the speed of 80 km/h

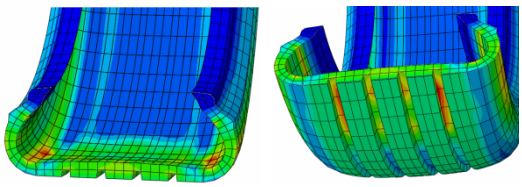

(e) Third stage: After 30 rotations at the speed of 80 km/h (cut-section)

Fig. 14. Temperature distribution within the rolling tire.

tire at different stages of the simulation. At the first stage (Fig. 14(a)), the tire comes in contact with the road. At this stage, no friction heat is generated, only minimal internal heat. Fig. 14(b) shows the temperature distribution at the cut-section, in which the outer part of the sidewall bends and internal heat is concentrated at the bended region of the shoulder tread block. In addition, the temperature at which the sidewall meets the tread is increased. At the second stage (Fig. 14(c)), the tire starts rolling. At this stage, heat is generated by friction between the tire and road, and the temperature of the tread that comes in contact with the road is the highest. Fig. 14(d) shows the temperature distribution within the rolling tire after 30 rotations at the speed of 80 km/s. The maximum temperature rise is 1 °C. The details of the temperature distribution within the tire is shown in Fig. 14(e). The left-hand side of Fig. 14(e) shows that heat is concentrated at the point where the sidewall meets the tread, which is similar to that of Fig. 14(b). The right-hand side of Fig. 14(e) shows the inside part of the tread block having a higher temperature than the outside part. This phenomenon can be explained by the convection applied to the outside part only of the tread block. The simulation results show that friction and internal heat can be generated successfully. Therefore, the proposed user subroutine and simulation method are both reliable.

4. Conclusions

A simulation method was proposed in this study to predict the temperature distribution within a 3D rolling tire. A user subroutine was developed in Abaqus to model the internal heat generation resulting from the hysteresis loss of rubber. A tensile test for the rubber specimen was conducted in thermal chamber conditions. Then, the obtained nominal stress-strain curve data were applied directly to the tensile simulation mod-

el based on the Marlow model. The reliability of the proposed user subroutine and corresponding method was verified by comparing the nominal stress-strain curves obtained from simulation and experiments at different temperatures. A simplified tire model that consisted of four solid parts and four membrane parts was developed. When the tire started to roll, the friction heat between the tire and the road and the internal heat caused by deformation were both generated. As the tire continuously rolled, the temperature distribution of the tire model changed. Heat was concentrated at the point where the sidewall meets the tread and the inside part of the tread block. This study is the first attempt to successfully simulate heat generation in actual rolling tire conditions by using an implicit dynamic solver. In the future, the temperature rise within a tire under cornering and braking conditions will be studied.

Acknowledgments

This work was part of a research program supported by the Ministry of Trade, Industry, and Energy (an R&D and infrastructure construction project to advance brand of high performance vehicle and parts), South Korea.

References

[1] T. G. Ebbott, R. L. Hohman, J. P. Jeusette and V. Kerchman, Tire temperature and rolling resistance prediction with finite element analysis, *Tire Science & Technology*, 27 (1) (1999) 2-21.

[2] K. K. Kar and A. K. Bhowmick, Hysteresis loss in filled rubber vulcanizates and its relationship with heat generation, *Journal of Applied Polymer Science*, 64 (8) (1997) 1541-1555.

[3] D. M. Park, W. H. Hong, S. G. Kim and H. J. Kim, Heat generation of filled rubber vulcanizates and its relationship with vulcanizate network structures, *European Polymer Journal*, 36 (2000) 2429-2436.

[4] H. C. Park, S. K Youn, T. S. Song and N. J. Kim, Analysis of temperature distribution in a rolling tire due to strain energy dissipation, *Tire Science & Technology*, 25 (3) (1997) 214-228.

[5] Y. J. Lin and S. J. Hwang, Temperature prediction of rolling tires by computer simulation, *Mathematics and Computers in Simulation*, 67 (2004) 235-249.

[6] A. R. Johnson, Coupled thermo-mechanical analysis of dynamically loaded rubber cylinders, *Proc. of 32nd International SAMPE Technical Conference*, Boston, USA (2000).

[7] Q. Kan, G. Kang, W. Yan, Y. Zhu and H. Jiang, A thermo-mechanically coupled cyclic plasticity model at large deformations considering inelastic heat generation, *Proc. of 13th International Conference on Fracture*, Beijing, China (2013).

[8] R. K. Luo, X. P. Wu and A. Spinks, Heat generation analysis of a rubber wheel using the steady-state transport analysis capability in abaqus, *Proc. of SIMULIA Customer Conference*, London, England (2009).

[9] T. Tang, D. Johnson, E. Ledbury, T. Goddette and S. D. Felicelli, Simulation of thermal signature of tires and tracks, *Proc. of Ndia Ground Vehicle Systems Engineering and Technology Symposium*, Michigan, USA (2012).

[10] R. S. Marlow, A general first-invariant hyperelastic constitutive model, *Proc. Of 3rd European Conference on Constitutive Models for Rubber*, London, England (2003).

[11] T. V. Korochkina, T. C. Claypole and D. T. Gethin, Choosing constitutive models for elastomers used in printing processes, *Proc. of 4th European Conference on Constitutive Models for Rubber*, London, England (2005).

[12] *Abaqus user's manual 6.11*.

Hyun Seok Song received his B.S. Mechanical Engineering from Ajou University in 2000. Currently, he is a Ph.D. candidate at Ajou University, and he is working at KATECH in Korea. Mr. Song's research interests are in the area of multi-body and structural dynamics, optimization, and computer-aided engineering.

Sung Pil Jung received his Ph.D. in Mechanical Engineering from Ajou University in 2010. His major is multi-physics simulation based on multibody dynamics. At present, he is working at KATECH as a Senior Researcher. Dr. Jung's research interests are chassis design, analysis, and testing.

Tae Won Park received his B.S. Mechanical Engineering from Seoul University. He received his M.S. and Ph.D. from the University of Iowa. Currently, Dr. Park is a Professor at the School of Mechanical Engineering at Ajou University in Suwon, Korea.